

# Ocean noise field-calibration constraints for deep sea mining

1<sup>st</sup> Luciano de Oliveira Júnior  
LARSyS, University of Algarve  
8005-139 Faro, Portugal  
lojunior@ualg.pt

2<sup>nd</sup> Orlando C. Rodríguez  
LARSyS, University of Algarve  
8005-139 Faro, Portugal  
sjesus@ualg.pt

3<sup>rd</sup> Sérgio M. Jesus  
LARSyS, University of Algarve  
8005-139 Faro, Portugal  
orodrig@ualg.pt

**Abstract**—The EU Horizon project TRIDENT aims at developing a comprehensive study to improve the understanding of the activities related to deep sea mining as well as to develop observation methodologies, technologies required for impact forecast, and possible mitigation measures. In the framework of TRIDENT, the impact of the acoustic field will be assessed by deploying a fixed array of acoustic recorders in the surrounding of the mining activity on top of the Tropic Seamount to monitor the near field, while acoustic gliders equipped with hydrophones will provide the observations from the far field. In complement, noise models will be routinely used for predicting sound distribution requiring frequent calibration with field data with a suitable spatial coverage. This work proposes a methodology and tests the calibration capabilities for ocean noise modelling in the context of DSM activities, where the main objective is to define the best sampling strategy for a glider to record data for calibrating acoustic propagation models. The analysis of the broadband transmission loss from contrasting oceanographic conditions allowed the identification of regions of interest assuring the best use of the acoustic glider in the upcoming sea trial.

**Index Terms**—acoustic calibration, deep sea mining, ocean noise, soundscape, glider.

## I. INTRODUCTION

Renewable energies, electric cars, and other "green" commodities show an increasing need for rare materials, which can not be found in sufficient quantity on land and justify for the economic viability of the exploitation of the deep ocean seabed [1]. Numerous initiatives were launched showing the probable environmental and ecosystem impact of deep sea mining [2, 3]. There at least two major potential consequences of deep sea mining (DSM): sediment plumes and energy input into the ocean. Energy input into the ocean is mostly achieved through machinery generated noise, vibrations and light [4]. Light impact is expected to be very localized at the mining site, due to the poor propagation of light underwater. Instead, mechanical vibrations and noise will most certainly propagate through the water column and into the sediment strata spreading vertically and horizontally according to the frequency range, amplitude and position of the excitation, and the physical properties of the media.

EU Horizon project TRIDENT aims at developing a comprehensive study to improve the understanding of the processes at play, observation methodologies, technologies and tools

Funded under project TRIDENT, European Union's HE program, grant agreement No 101091959.

required for impact forecast, activity monitoring and possible mitigation measures [5]. TRIDENT's activity and system demonstration will take place at the Tropic seamount (TSM), located to the south of Canary Islands (Fig. 1a).

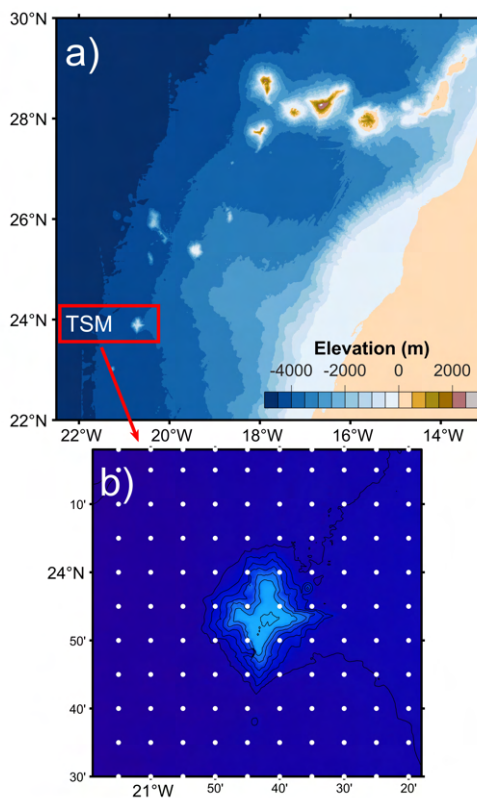


Fig. 1. a) GEBCO bathymetry of surroundings of the Canary Islands and Tropic Seamount location. b) Copernicus grid (white dots) and Tropic Seamount bathymetry represented with 500m contour intervals from 4500 m depth.

Within the TRIDENT framework, the acoustic field will be assessed through observational approach by deploying a fixed array of acoustic recorders in the surrounding of the mining activity on top of the TSM to monitor the near field, while acoustic gliders equipped with hydrophones will provide the observations from the far field. In complement, noise models will be routinely used for predicting sound distribution. These models are based on acoustic propagation numerical codes

fed with marine traffic information from AIS, bathymetry, temperature and wind data from data bases.

Free running noise prediction models are inherently biased and divergent along time, mostly due to limited and inaccurate input data. This prompts for frequent model calibration with field data with a suitable spatial coverage. This work studies, develops methodologies and tests the calibration capabilities for ocean noise modelling in the context of DSM activities. The main objective is to define the best sampling strategy for a glider to record data for calibrating acoustic propagation models.

## II. DATA AND METHODS

### A. Data

Historical daily averages Temperature and Salinity data provided by Copernicus (GLOBAL\_ANALYSISFORECAST\_PHY\_001\_024-TDS) were used to compute sound speed following [6, 7] in an area of approximately 200 km by 200 km centered at the TSM (black dots in Fig. 1). The data set covers the period between November 2020 to January 2024.

Ocean noise propagation is simulated using BELLHOP3D considering two distinct sound speed scenarios. The two distinct scenarios were selected in order to capture the system largest (temporal and spatial) variability so the calibration methodology can be tested within reasonable values despite the lack of observational data. The chosen scenarios were named “True” and “Variable”, and were obtained as follows: First, Empirical Orthogonal Functions (EOFs) were computed, and the data set was reconstructed from the modes that accounted together for 90% of the total explained variance. Subsequently, the “True” and “Variable” scenarios were obtained by computing the average of all available data for the periods between September-October and February-March consecutively. The above criteria was chosen based on the temporal distribution of EOF mode 1 which indicates that the system largest differences occur between Winter and Summer (See Fig. 2a). To validate the profiles reconstructed with the method described above, Temperature and Salinity data from in situ observations at the study site were used to compute the sound speed and is presented in Fig. 2b-c. Observations were obtained during the JC142 cruise from National Oceanography Centre during October-December 2016 around the TSM [8] and the profiles for the True and Variable scenario were extracted from a longitudinal transect centred at the top of the TSM. It is possible to observe that overall, an agreement is achieved in terms of the magnitude and depth distribution of the sound speed. A better agreement is obtained for the True scenario due to the similar period of the year that the observed data was collected. The largest discrepancies between observations and the reconstructed profiles, are observed near the surface due to the surface stratification present during summer period (represented by the Variable scenario).

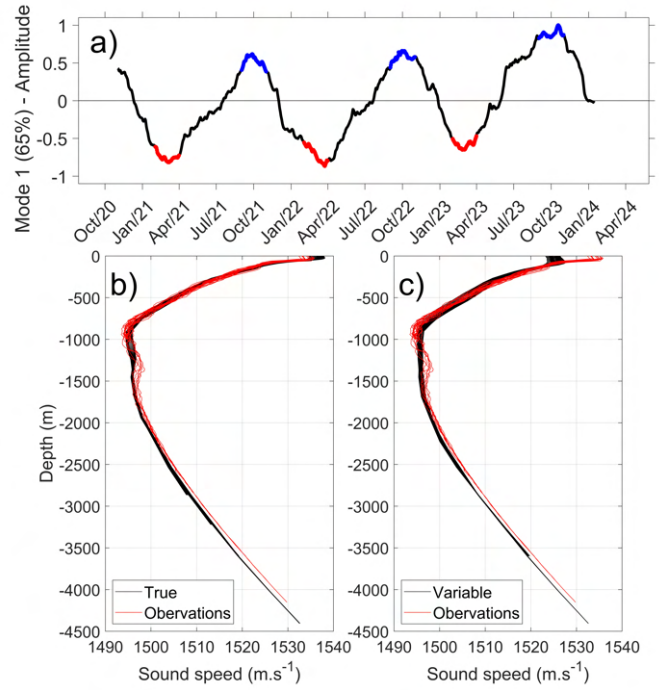


Fig. 2. a) Normalized amplitude of EOF mode 1 (black) and the contrasting periods used for computing the True (blue) and Variable (red) scenarios. Sound speed profiles for the True (b) and Variable (c) scenario in black and sound speed profiles from observations around the TSM in red.

### B. Acoustic propagation model and Sampling Strategy

Transmission loss (TL) from the True and Variable scenarios was calculated using the BELLHOP3D Gaussian beam acoustic model [9]. The broadband field is calculated as the sum of the received relative pressure power at the center frequencies of one third octave frequency bands in the interval 12 Hz - 4 kHz. This calculation was performed for source depths of 5, 500, and 1022 m, which are considered representative depths for the surface vessels, a pump of the riser system, and for the mining vehicle operating on the top of the Tropic Seamount, respectively. Finally, properties of a sandy bottom were taken from [10].

First, the broadband TL field will be presented for the True and Variable cases. This is an important step as it will indicate regions where noise from the DSM activity is expected to be relevant. Second, the TL differences between of the True and the Variable fields will indicate which are the regions where most contrasting conditions occur. Therefore, those regions are of most interest to be sampled for calibration purposes as models are expected to have a higher degree of failure in these regions.

Model results will be sampled by a simulated acoustic glider dive following the specifications of the ALSEAMAR Sea Explorer X2 glider which will be used in the sea trials during the activities of TRIDENT. Dives should not exceed a 30° dive angle (relative to the surface) and not exceed the 1000 m depth. TRIDENT sea trial will be performed during 10 days,

which represent an approximate maximum distance of 100 km for a glider mission. The optimization of the calibration is achieved by testing several sampling strategies in terms of dive profiles that prioritizes the regions of interest. This is an important step as it will indicate the best setting for the in-situ observations (performed by acoustic gliders) and sets the stage for determining the actual expected field calibration performance or, at least, its performance upper bound.

The strategy must also take into account the mining activity itself, as the glider is an essential tool for the real time and long-range monitoring system. In the end, the best strategy must cover regions where both True and Variable scenarios differ the most and where noise from mining activity is expected to be relevant. Finally, the results of the 3D model will be assessed by comparing the results from a longitudinal transect (EW transect) against a latitudinal transect (NS transect) both centred at the top of the TSM.

### III. RESULTS

Overall TL is minimal around the TSM (approximately 10-20km radius) from the surface to the top of the seamount to form a principal lobe (Fig. 3). The SOFAR region (1000-1500 m depth) also present relatively low energy loss for all cases. Away from the top, there is a well-known shadow-convergence zone. The surface convergence zones occur approximately 60-80 km away from the mountain top and the regions with highest TL (shadow zones) are found between 20 and 40 km away from the sources (represented by the black dots) and are confined between the surface and 1000m. An exception to this overall pattern is found at the western flank of the seamount for the True scenario (Fig. 3a) where the convergence zone is not well defined, and the region of lowest energy loss is found between 1000 and 2500 m depth.

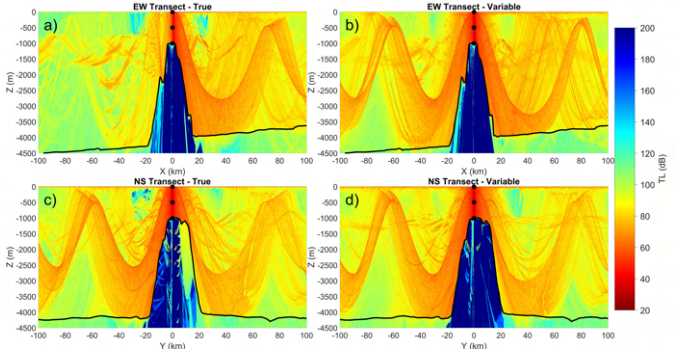


Fig. 3. Broadband Transmission loss (TL) field for the center frequencies of one third octave band in 12 Hz-4kHz. Black line represents the bathymetry and black dots represent the position of the sources. True and variable transect are represented in a) and b) for the EW transect and in c) and d) for the NS transect.

Regarding the TL differences between True and Variable scenarios (Fig. 4), the highest values are generally found 20 to 60 km away from the noise sources in the regions where TL is generally high (Fig. 3). The highest values of TL differences are found at the Northern flank (Fig. 4b) of the seamount

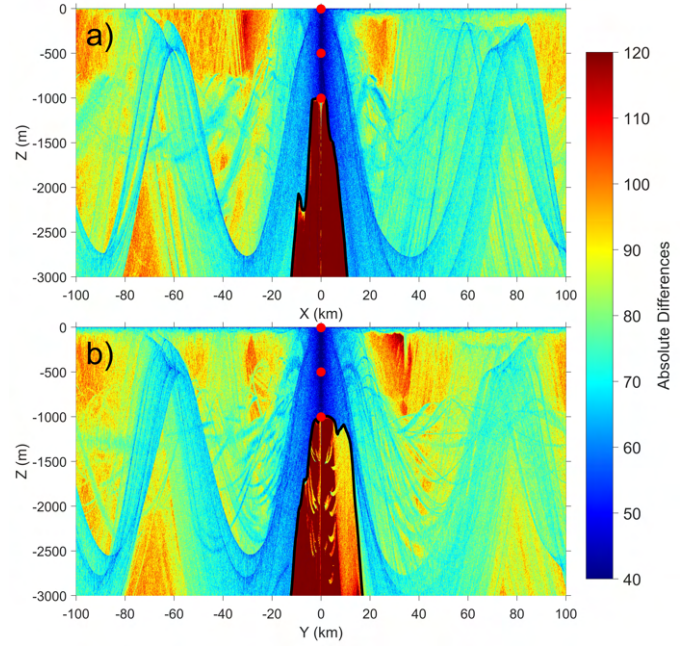


Fig. 4. Absolute TL differences between true and variable scenarios for the EW transect (a) and NS transect (b). Black line represents the bathymetry and red dots show the position of the noise sources

within a narrow band of values  $\geq 120$  dB between 30 and 40 km from 100m depth to 1000 m depth. However, the western flank (Fig. 4a) presents a larger area with values  $> 100$  dB going from 20 to 60 km and from 90 to 100 km, which makes this region more interesting to sample in the context of the calibration of the acoustic propagation model.

With the regions of highest differences being identified, in the following it will be tested which sampling strategies will better cover those regions. The dive types to be tested will cover regions 10 km away from the sources and further, varying the angle of dives at the regions of more or less interest (Fig. 5). Profiles 1 and 2 have fixed dive angles of  $26^\circ$  and  $21^\circ$  that results in 4 and 5 km distance between each surface point, respectively. Profile 3 has a dive angle of  $21^\circ$  at the first 15 km, after the angle is increased to  $26^\circ$ . In the following profiles (4-7), combination of large angles (e.g.  $26^\circ$  and  $21^\circ$ ) are only used for the regions where TL differences are large, whereas small angles are used to avoid regions where TL differences are generally low.

To quantify the performance of each sampling strategy, the mean of the differences sampled along each dive is plotted in Fig. 6 for the western flank of EW transect (in black) and for the northern flank of the NS transect (in red). Regardless of the dive patterns, the mean sampled differences at the western flank are always larger than at the northern flank, supporting that glider dives should be made towards the west. The dive types that avoid regions with low TL differences (i.e. profiles 5, 6 and 7) perform similarly well on both transect, but profile 6 at the EW transect indicate that this is the optimal strategy for the gliders to follow. Nevertheless, dive 7 is mainly

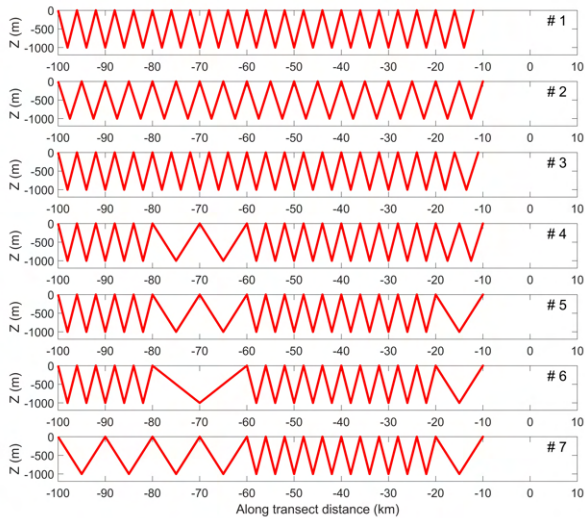


Fig. 5. Different types of Glider dives, 1 to 7 from top to bottom with variable dive angles.

focused on the region between the 20 to 60 km, yet the mean difference is slightly lower than for dive profile 6 indicating that regions further away are of secondary importance. Despite this exercise is performed considering only 2 transect of a 3D volume for the sake of simplicity and to aid with the visualization, in reality the gliders could perform dives in any direction. Thus, in the light of the present results, that indicate that the largest TL differences occur within the region of 20 - 60 km away from the mountain top and independently of the transect, the best sampling strategy should be performed in a circular way with a 30 to 40 km radius from west to north (or vice versa), within the beginning and end of a mission at the 10 km mark.

It is noted that in this paper, shipping and wind noise is omitted for simplicity, but the inclusion of those variables is foreseen for a more realistic representation. Furthermore, instead of absolute TL, realistic noise source level values from DSM activity should be assigned to each specific frequency as in [11]. This will probably exclude regions where DSM noise would never be achieved, thus refining the glider sampling strategy for both monitoring and calibration purposes.

#### IV. CONCLUSIONS

This paper presents a methodology for defining a best sampling strategy for a glider mission used for acoustic field-calibration purposes within the activities of the TRIDENT project. The chosen strategy is proposed taking into account the mining activity itself, as the glider is an essential tool for the real time and long-range monitoring system and also considering regions of largest variability where the acoustic propagation model is expected to have a higher degree of failure. The analysis of the broadband TL field at a longitudinal and latitudinal transects for two contrasting oceanographic

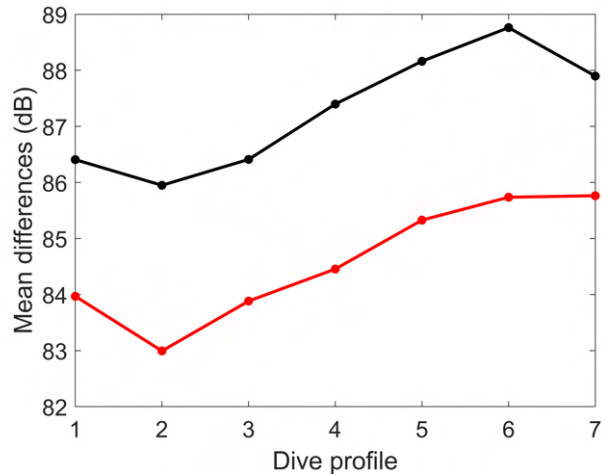


Fig. 6. Mean TL differences sampled along each dive profile at the EW transect (in black) and at the NS transect (in red).

conditions allowed for the identification of regions of interest and indicated the actual expected field calibration performance.

Results show that around the TSM region, the variability of sound propagation is largest between the main lobe and convergence zones for depths up to 1000 m in both longitudinal and latitudinal transects, being the eastern flank of the TSM the region of most interest. However, the final strategy proposed here refer to a glider dive that should be performed in a circular way with a 30 km to 40 km radius preferably within the NW quadrant.

#### ACKNOWLEDGMENT

This work was performed under TRIDENT project that has received funding from the European Union's HE programme under grant agreement No 101091959.

#### REFERENCES

- [1] James R. Hein, A. K. T. A. C., Kira Mizell. Deep-ocean mineral deposits as a source of critical metals for high- and green-technology applications: Comparison with land-based resources. *Ore Geology Reviews* **51**, 1–14 (2013).
- [2] Ramirez-Llodra, E. *et al.* Man and the last great wilderness: Human impact on the deep sea. *PLoS ONE* **6** (2011).
- [3] Chin, H. K., A. Predicting the impacts of mining of deep sea polymetallic nodules in the Pacific Ocean: A review of scientific literature. *Deep Sea Mining Campaign and MiningWatch Canada* (2020).
- [4] Cyrill Martin; Dr. Lindy Weilgart; Dr. Diva J. Amon; Dr. Johannes Müller, O. *Deep-Sea Mining: A noisy affair*, vol. 1 (oceanare, 2021).
- [5] E.Silva; D.Viegas; A.Martins; J.Almeida; C.Almeida; A., B.Neves; P.Madureira. Trident – technology based impact assessment. Tech. Rep., TRIDENT (2023).

- [6] Mackenzie, K. V. Nine-term equation for sound speed in the oceans. *Journal of the Acoustical Society of America* **70**, 807–812 (1981).
- [7] Mackenzie, K. V. Discussion of sea water sound-speed determinations. *Journal of the Acoustical Society of America* **70**, 801–806 (1981).
- [8] Research, H. Marine-tech project to map cobalt-rich ferromanganese crusts of tropic seamount, ne atlantic. Tech. Rep., NOC (2016).
- [9] Porter, M. Bellhop3d user guide. technical report. Tech. Rep., HLS Research (2016).
- [10] Finn B. Jensen, M. B. P. H. S., William A. Kuperman. *Computational Ocean Acoustics*, vol. 1 (Springer Science, 2011).
- [11] Jesus, S. M. & Rodríguez, O. C. Estimating excess noise from deep sea mining: a simulated test case. In *OCEANS 2023 - Limerick*, 1–6 (2023).